Prediction of Atherosclerotic Plaque Development in an in Vivo Coronary Arterial Segment based on a multi-level modeling approach

Antonis I. Sakellarios, Lorenz Räber, Christos V. Bourantas, Themis P. Exarchos, Lambros S. Athanasiou, Gualtiero Pelosi, Konstantinos C. Koskinas, Oberdan Parodi, Katerina K. Naka, Lampros K. Michalis, Patrick W. Serruys, Hector M. Garcia Garcia, Stephan Windecker, Dimitrios I. Fotiadis *Senior Member, IEEE*

***Abstract*— *Objective:* The aim of this study is to explore major mechanisms of atherosclerotic plaque growth, presenting a proof-of-concept numerical model. *Methods:* To this aim, a human reconstructed right coronary artery is utilized for a multi-level modeling approach. More specifically, the first level consists of the modeling of blood flow and endothelial shear stress (ESS) computation. The second level includes the modeling of low and high density lipoprotein (LDL, HDL) and monocytes transport through the endothelial membrane to vessel wall. The third level comprises of the modeling of LDL oxidation, macrophages differentiation and foam cells formation. All modeling levels integrate experimental findings to describe the major mechanisms that occur in the arterial physiology. In order to validate the proposed approach, we utilize a patient specific scenario by comparing the baseline computational results with the changes in arterial wall thickness, lumen diameter and plaque components using follow-up data. *Results:* The results of this model show that ESS and LDL concentration have a good correlation with the changes in plaque area [R2=0.365 (P=0.029, adjusted R2=0.307) and R2=0.368 (P=0.015, adjusted R2=0.342), respectively] whereas the introduction of the variables of oxidized LDL, macrophages and foam cells as independent predictors improves the accuracy in predicting regions potential for atherosclerotic plaque development [R2=0.847 (P=0.009, adjusted R2=0.738)]. *Conclusion:* Advanced computational models can be used to increase the accuracy to predict regions which are prone to plaque development. *Significance:* Atherosclerosis is one of leading causes of death worldwide. For this purpose computational models have to be implemented to predict disease progression.**

***Index Terms*— Atherosclerotic plaque growth, finite elements, prediction of plaque growth, proof-of-concept study**

08/07/2016. "This work is partially funded by the European Commission (Project ARTREAT: Multi-level patient-specific artery and atherogenesis model for outcome prediction, decision support treatment, and virtual hand-on training, FP7-224297, Project SMARTOOL, GA number: 689068, H2020)".

A.I. Sakellarios and D.I. Fotiadis are with the Unit of Medical Technology and Intelligent Information Systems, Dept. of Materials Science and Engineering, University of Ioannina, GR 45110 (email: ansakel@cc.uoi.gr, correspondence phone: +302651009906; e-mail: fotiadis@cc.uoi.gr).

A.I. Sakellarios, T. Exarchos and D.I. Fotiadis are with the Dept. of Biomedical Research, Institute of Molecular Biology and Biotechnology – FORTH, University Campus of Ioannina, 45110, Ioannina, Greece (email: themis.exarchos@gmail.com).

L. Räber, K. Koskinas and S. Windecker are with the Dept. of Interventional Cardiology, Bern University Hospital, Bern, Switzerland (email: Lorenz.Raeber@insel.ch; Stephan.Windecker@insel.ch).

C. Bourantas is with the Department of Cardiovascular Sciences, University College London, UK (email: cbourantas@gmail.com).

L. Athanasiou is with the Cardiovascular Division, Brigham and Women's Hospital, Harvard Medical School, Boston, USA (email: lambros@mit.edu).

G. Pelosi and O. Parodi are with Institute of Clinical Physiology, National Research Council, 56124, Pisa, Italy (email: pelosi@ifc.cnr.it; oberdan.parodi@virgilio.it).

K.K. Naka and L.K. Michalis are with the Michaelideion Cardiac Center, Dept. of Cardiology in Medical School, University of Ioannina, GR 45110 Ioannina, Greece (email: anaka@cc.uoi.gr, lmihalis@cc.uoi.gr).

P. Serruys is with the Dept. of Interventional Cardiology, Erasmus MC, Thoraxcenter, Rotterdam, The Netherlands (email: patrick.w.j.c.serruys@gmail.com).

H. Garcia-Garcia is with the Dept. of Interventional Cardiology, MedStar Washington Hospital Center, Washington, DC, USA (email: hect2701@gmail.com).

I. Introduction

In western societies, 30% of deaths is caused by coronary artery disease (CAD) [1]. Several systemic factors appear to regulate atherosclerotic evolution including hypertension, hyperlipidemia, chronic inflammation and diabetes. These biochemical factors attract monocytes. Consequently, the monocytes are modified to macrophages, which phagocyte the molecules of oxidized LDL (LDLox). Inefficient macrophage phagocytosis, modified LDL accumulation and cell apoptosis/necrosis, drive the formation of the lipid-necrotic core of the plaque, which, in combination with smooth muscle cell proliferation, characterize the high-risk complicated and/or flow obstructing plaques.

Though atherosclerosis is a systemic disease, its pathologic expression and clinical manifestations are site-specific. Several local mechanisms may be responsible for this artery/site-specificity. In fact, low ESS and LDL accumulation and oxidation triggers vascular inflammation and promotes the expression of several chemotactic molecules and cytokines. Experimental and clinical studies have shown that rheology and especially low ESS play a considerable role in plaque

growth and development[2]. More specifically, complex arterial regions such as the bifurcations or the curved arteries presenting low ESS and disturbed flow are more prone to plaque growth. It has been shown in dedicated mechanistic studies that low ESS affects endothelial membrane by altering locally the gene expression [3], as well as its permeability [4, 5].

Computational modeling has provided insights into atherosclerotic plaque development. Initial approaches focused on the simulation of blood flow in order to clarify the effect of ESS on plaque growth. Several studies reported a strong correlation between low ESS and plaque development [6, 7], while the recently published PREDICTION study demonstrated that low ESS is associated not only with an increased risk for plaque development but also with future cardiovascular events [8].

More recently, studies attempted to model complex mechanisms of atherosclerosis, such as the macromolecular transport. Computational studies on LDL transport attempted to simulate the mechanisms of LDL accumulation into the arterial wall which can be considered as the initial step, from the biological point of view, of plaque formation. Several studies have been carried out on LDL transport which can be categorized into: (i) studies where the endothelial membrane was considered as non-permeable [9, 10], (ii) studies wherein the endothelial membrane is semi-permeable and the arterial wall is structured as one homogenous cell layer [11-15], and (iii) studies which consider the arterial wall as multi-layer [16-18]. In the majority of these studies the endothelial membrane is considered as an active barrier which reacts to ESS [13, 19], hypertension [18, 20] or biological conditions, e.g. the nitric oxide (NO) concentration [21] or the mitosis of endothelial cells [12, 22, 23]. Finally, the most recent studies by Filipovic *et al*. [24, 25] simulated several steps of plaque growth from blood flow and LDL transport to macrophages and foam cells formation.

In this work, we present a novel model for plaque growth prediction. Our approach is based on a multi-level modeling rationale: first images from intravascular ultrasound (IVUS) and angiography are utilized to reconstruct the coronary artery, ii) blood flow is modeled and the ESS is calculated, iii) LDL, HDL and monocytes transport is modeled considering the effect of ESS and iv) plaque growth modeling is performed. This level consists of the oxidation of LDL under the protective effect of HDL, the differentiation of macrophages and finally foam cells formation.

The innovation of the proposed model is that it considers all the main biological and biochemical mechanisms of plaque growth such as the oxidation of LDL, the recruitment of monocytes and the formation of foam cells. In addition, for the first time, information about plaque characteristics acquired from images at one time point is integrated in the mathematical model. More specifically, macrophages accumulation is depicted in optical coherence tomography (OCT) frames and the findings are integrated as boundary condition in the proposed model. Last but not least, we present a validation scenario of the model by examining the computational results acquired from baseline medical examinations with the follow-up virtual histology (VH) findings of plaque components as well as with the follow-up OCT findings of macrophages. Part of this work was previously presented [26], however the abovementioned innovations characterize only this work.

The results of a proof of concept experimental study in the hypercholesterolemic swine model of atherogenesis are also included as a validation scenario of the association between inflammatory and morphological features of coronary lesions and ESS values.

II. Materials and Methods

A. Patient's data and 3D reconstruction

A patient was admitted with an acute coronary syndrome, had revascularization and was recruited for the IBIS 4 study [27]. As part of the study protocol he underwent IVUS-VH and OCT imaging in the non-treated vessels at baseline and after 13 months follow-up (Table 1).

TABLE I
Virtual Histology (VH) Analysis of Reconstructed Arterial Segment.

Plaque Analysis	Baseline	Follow-up	% Difference
Fibrous Volume (mm^3)	3.26	3.76	15.34
Fibrous Fatty Volume (mm^3)	0.54	0.44	-18.52
Necrotic Core Volume (mm^3)	1.07	1.70	58.89
Dense Calcium Volume (mm^3)	0.25	0.40	60
Plaque Volume (mm^3)	4.13	4.03	-2.42

Fig. 1 shows the angiographic, IVUS and OCT images for baseline and follow-up time points. Written informed consent was obtained from the patient for using the data for research purposes.

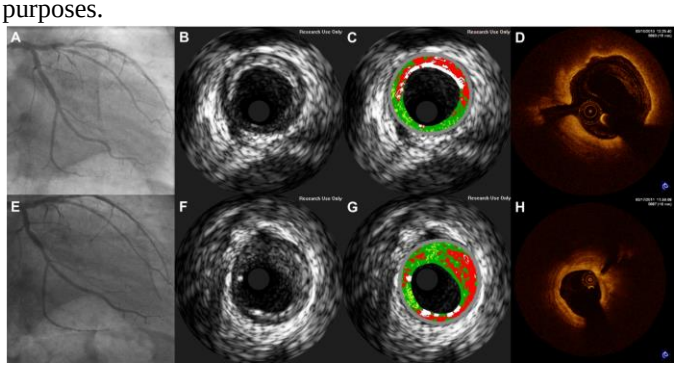

Fig. 1. (A-D) and (E-H) depict baseline and follow-up imaging, respectively. (A, E) Coronary angiography shows an LCX artery with two stenosed regions at the follow-up examination. (B, C, F, G) the IVUS examination at the bifurcation region and the corresponding virtual histology examination. (D, H) The corresponding OCT examination with increased plaque at the follow-up examination.

Coronary artery reconstruction was performed using a validated methodology based on the fusion of angiographic and IVUS data as previously described [28]. Briefly, the catheter path was extracted from Biplane angiographic images. Finally, the luminal and media-adventitia borders were detected in IVUS and they were placed onto the catheter path and their absolute orientation was estimated. The final

results represent the lumen and adventitia surfaces (Fig. 2).

B. Animal studies

In 12 pigs on high fat high cholesterol diet, an IVUS catheter (20 MHz,100, 200 μm axial resolution, 5 mm penetration) has been advanced in distal left anterior descending artery (LAD), coronary Doppler flow velocity measured, and resulting 2D tomographic sections were used to obtain 3D reconstruction for ESS estimate. Animal instrumentation and experimental protocol were approved by the Animal Care Committee of the Italian Ministry of Health and were in accordance with the Italian Law (DL-116, Jan. 27, 1992), which is in compliance with the National Institute of Health publication Guide for the Care and Use of Laboratory Animals.

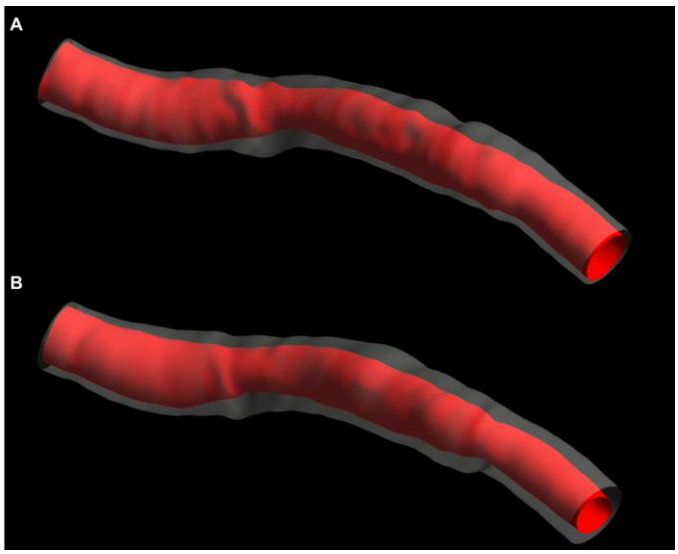

Fig. 2. (A) 3D reconstructed left circumflex artery at the baseline time point (red color: lumen; transparent grey color: outer wall). (B) 3D reconstructed coronary artery at the follow up time point (red color: lumen; transparent grey color: outer wall).

ESS coronary profiling was obtained before and after 2 and 4 months hypercholesterolemic diet. The main coronary arteries were examined by histology and immunohistochemistry (IHC). Blood samples were collected at baseline and end diet for measuring lipoprotein concentration and inflammatory markers. Quantitative IHC was used to assess immune-expression of several relevant markers of monocyte activation/migration and of foam cells, including macrophage migration inhibitory factor (MIF), stromal derived factor 1a (SDF1a) chemokine receptor type 4 (CXCR4) and calprotectin (MAC387, S100A8/A9), a classic macrophage marker [29].

C. Modeling blood flow

We assume that blood flow is laminar and incompressible while blood behaves as a Newtonian fluid. Blood flow in the arterial lumen was modeled using the Navier-Stokes equations and the continuity equation:

$$-\mu\nabla^2\mathbf{u}_l + \rho\left(\mathbf{u}_l\cdot\nabla\right)\mathbf{u}_l + \nabla p_l = 0, \quad (1)$$

$$\nabla\cdot\mathbf{u}_l = 0, \quad (2)$$

where l refers to the lumen, $\mathbf{u}_l$ is the blood velocity, p_l is the pressure, μ is the dynamic viscosity of blood, and ρ is the blood density.

Plasma filtration in the arterial wall was modeled using Darcy's Law assuming that arterial wall is a homogenous porous media:

$$u_w - \nabla\cdot\left(\frac{\kappa_w}{\mu_p}p_w\right) = 0, \quad (3)$$

where p_w is the pressure in the arterial wall and u_w is the plasma velocity, μ_p is the plasma viscosity and k_w is the Darcian permeability.

D. Modeling plaque growth

Plaque growth is modeled considering the main pathophysiological processes which occur during atherosclerotic plaque development: i) LDL, HDL and monocytes transport, ii) LDL oxidation, iii) macrophage differentiation and iv) foam cell formation.

We modeled LDL, HDL and monocyte transport in the arterial lumen using the convection-diffusion equations:

$$\nabla\cdot\left(-D_{l,LDL}\nabla c_{l,LDL} + c_l u_{l,LDL}\right) = 0, \quad (4)$$

$$\nabla\cdot\left(-D_{l,HDL}\nabla c_{l,HDL} + c_l u_{l,HDL}\right) = 0, \quad (5)$$

$$\nabla\cdot\left(-D_{l,monocytes}\nabla c_{l,monocytes} + c_{l,monocytes}u_{l,monocytes}\right) = 0, \quad (6)$$

where l indicates the lumen domain, *LDL*, *HDL* and *monocytes* the molecules or cells of LDL, HDL and monocytes, respectively. D is the diffusivity of each molecule or cell and c is the corresponding concentration.

Additionally, we model LDL transport in the arterial wall using a convection-diffusion-reaction equation:

$$\nabla\cdot\left(-D_{w,LDL}\nabla c_{w,LDL} + k c_{w,LDL}u_{w,LDL}\right) = r_{w,LDL}c_{w,LDL}, \quad (7)$$

where D_w is the diffusivity in the wall, r_w is the consumption rate constant and k is the solute lag coefficient.

LDL oxidation is modeled taking into account the athero-protective role of HDL. Previous data [30] are used for this purpose. Necessary fitting of the experimental data is made in order to represent physiological human values. Details about the LDL oxidation and the fitting of the experimental data can be found elsewhere [31]. The oxidation of LDL was modeled using a diffusion-reaction equation:

$$0 = \nabla\left(D_{OxLDL}\nabla c_{OxLDL}\right) + r_{w,LDL}c_{LDL} - k_1 M c_{OxLDL} - HDL_{protection}, \quad (8)$$

where c_{OxLDL} is the oxidized LDL concentration, D_{OxLDL} is a diffusion coefficient of oxidized LDL, k_1 is a constant absorption rate of macrophages to oxidized LDL and M is the number of macrophages. The equation requires as inlet boundary condition the calculated LDL concentration, while the reaction term of the equation takes into account the HDL concentration. $HDL_{protection}$ was defined by the experimentally observed relation shown in Fig. 3 and gives the oxidation rate of LDL molecules by the following equation:

$$HDL_{protection} = -3\text{x}10^{-5}c_{l,HDL}^{\ 2} + 0.0005c_{l,HDL} + 1.0056 \quad (9)$$

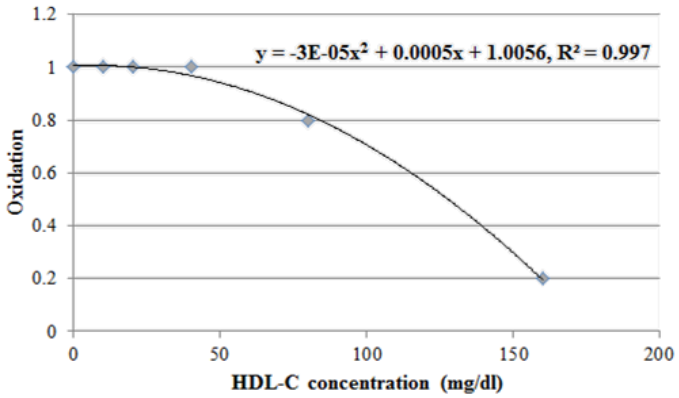

Fig. 3. Relation of LDL oxidation rate with HDL concentration. The fitting and the extraction of the relation is described in [16].

Finally, macrophage migration and foam cell formation are modeled using the following equations:

$$0 = \nabla\left(\rho D_M \nabla c_M\right) + \frac{c_s}{1+c_s} - k_1 M c_{OxLDL}, \quad (10)$$

$$0 = \nabla\left(\rho D_S \nabla c_S\right) + MIF, \quad (11)$$

$$\nabla v_w = k_1 M c_{OxLDL}, \quad (12)$$

where D_M and D_S are the diffusion coefficients for macrophages and cytokines, respectively. c_M and c_S are the macrophages and cytokines concentration, respectively. k_1 is the growing plaque coefficient.

E. Assumptions and boundary conditions

In the proposed model, we assume that Macrophage Migration Inhibitory Factor (MIF) expression depends on the lesion severity. This assumption is based on the results observed from the animal studies. More specifically, Fig. 4B depicts the relation of MIF with lesion area which is found and characterized by the expert at each histological frame Furthermore, lesion area is found to be correlated very well with total wall thickness as shown in Fig. 4A. Thus, using these relations, we are able to assume the local expression of MIF gene measured using polymerase chain reaction (PCR). Its concentration is applied as a boundary condition for the estimation of the cytokines concentration.

A novelty of this study is that it introduces for the first time the baseline macrophage accumulation, acquired from OCT images. After co-registration with IVUS images we integrate this information in our model. In order to perform this, we fit a function of macrophages accumulation as shown in Fig. 5 to receive the macrophage accumulation along the longitudinal distance. Then this function is multiplied with the boundary condition of the MIF concentration.

Another assumption of our model is that the oxidized LDL is responsible for monocyte differentiation to macrophages. This means that oxidized LDL increases vascular inflammation. In order to represent mathematically this relation of oxidized LDL with macrophages/monocytes we incorporate in our model a boundary condition which is extracted by the experimental findings of Hayden *et al.* [32].

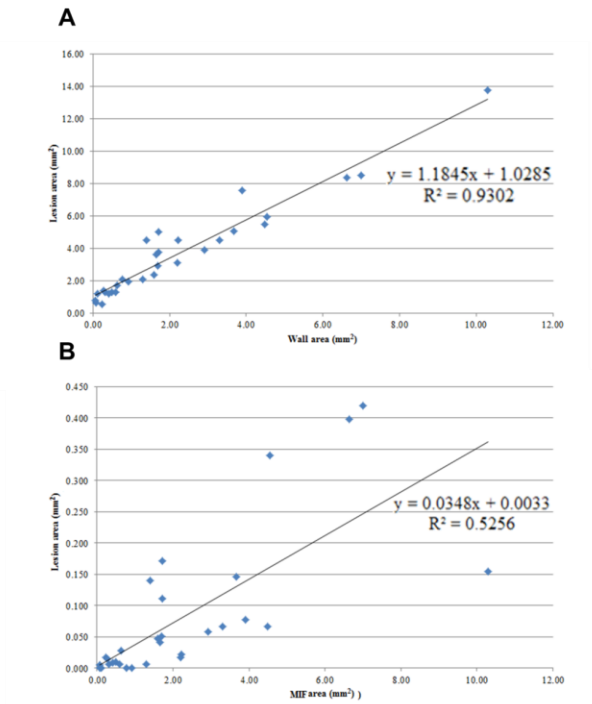

Fig. 4. Results from animal studies. (A) Relation of lesion area found in each histological section with total wall thickness as observed by histology, (B) relation of lesion area with measured MIF area.

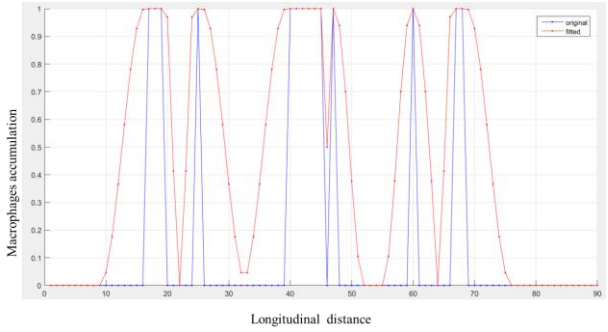

Fig. 5. The blue line shows the original macrophages accumulation along the longitudinal length of the arterial segment. The red line depicts the fitting function.

Fig. 6 presents this relation as well as the fitting curve. 7-ketocholesterol (7-KC) is found in relatively large abundance in OxLDL and for this reason we assume that OxLDL has a similar relation with monocyte differentiation. The diagram of Fig 6 shows that increased values of oxidized LDL increase the differentiation of monocytes to macrophages.

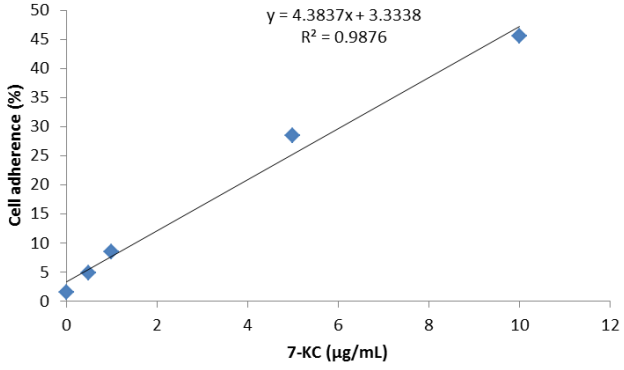

Fig. 6. Relation of macrophage adherence with the 7-KC component of oxidized LDL.

At the inlet boundary of the arterial segment a constant blood velocity was applied (u_0 = 129 mm/s). The boundary conditions applied for mass transport were a constant concentration for LDL particles ($C_{0,LDL}$ = 1.696×10^{-3} mol/m^3; corresponding to 160 mg/dl LDL-cholesterol in plasma) and HDL particles ($C_{0,HDL}$ = 0.636×10^{-3} mol/m^3; corresponding to 60 mg/dl HDL-cholesterol in plasma) at the inlet and the adventitia boundary (0.005$C_{0,LDL}$), and a convective flow at the outlet of the artery.

Kedem-Katchalsky equations [33] were used to model the interaction between the lumen and the arterial wall at the endothelial membrane layer for LDL, HDL and monocytes:

$$J_v = L_p\left(\Delta p - \sigma_d \Delta\pi\right), \quad (13)$$

$$J_s = P\Delta c + \left(1-\sigma_f\right) J_v \bar{c}, \quad (14)$$

where L_p is the hydraulic conductivity of the endothelium; Δc is the solute concentration difference (specific for any component transported in the lumen), Δp is the pressure drop and $\Delta\pi$ is the oncotic pressure difference, in the endothelium; σ_d is the osmotic reflection coefficient, σ_f is the solvent reflection coefficient, P is the solute diffusive endothelial permeability, and c is the solute concentration. In this study the oncotic pressure difference is neglected and thus the fluid dynamics are decoupled from solute dynamics. The diffusive endothelial permeability is calculated as described in Sakellarios et al. [20]. We assume that hydraulic conductivity depends on ESS according to the study of Sun *et al*. [14].

Finally, we assume that at the adventitia boundary, macrophages and cytokines concentration are zero, while at the endothelial boundary the monocytes transmigration is given as:

$$monocytes = 163.83e^{-0.133ESS},\ R^2 = 0.8351. \quad (15)$$

This relation is extracted from experimental data [34] and the fitted curve is shown in Fig. 7. In this study, it was shown that ESS affects the rolling, arrest and transmigration of monocytes. Moreover, this effect was quantified under several ESS conditions, which have been used for our model in order to measure the transmigrated monocytes based on the local ESS.

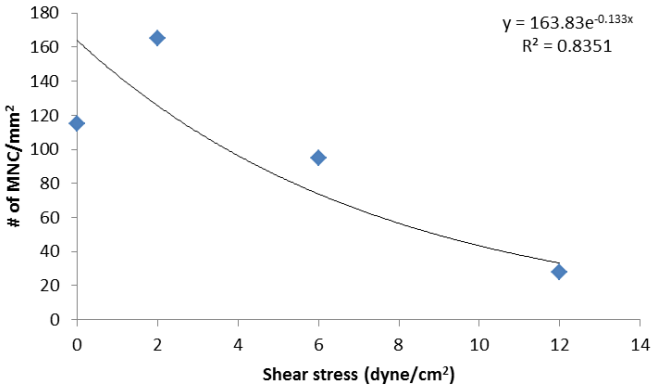

Fig. 7. Relation of shear stress with the number of adhered monocytes.

III. Results

Plaque size by standard histomorphometric indexes (i.e. intimal thickness (IT), and cross sectional lesion area (LA)), is inversely related to the value of baseline ESS at corresponding arterial sites both in all group segments and in single case individual artery (Fig. 8).

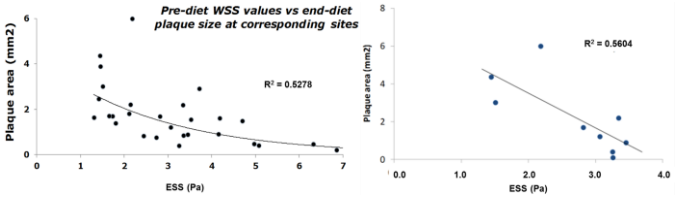

Fig. 8. Relation between baseline wall shear stress (WSS) and corresponding plaque cross sectional area in all segments of 4 months diet treated cases (left) and in the LAD artery of a single case (right).

Plaque size is also directly related with the degree of MAC387 positive macrophages and to the level of MIF-CXCR4 intra-lesion immune-expression, assessed as percent positive area of corresponding antibodies by quantitative immunohistochemistry (Fig. 9). These findings suggest that the involvement of the MIF-CXCR4 axis may contribute to the coronary atherosclerosis severity and extent in the hypercholesterolemic swine model.

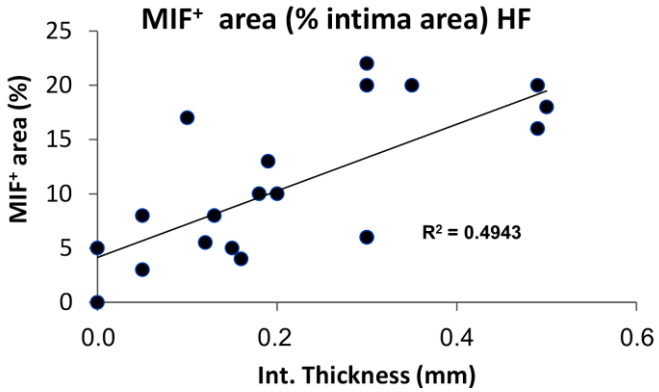

Fig. 9. Relation between plaque size index (mean intimal thickness) and intra-lesional MIF+ area at corresponding arterial sites in all segments of 2 months diet treated cases.

Simulation of plaque growth is performed at the baseline reconstructed arterial segment and the baseline modeling results are compared with the change of lumen, plaque burden and composition at follow-up. This is performed by segmenting the 3D model into segments of 0.5 mm. The mean values (areas) of each plaque component observed in each frame located in the corresponding segment are calculated.

An inverse relation between ESS and LDL concentration was found as it is shown in Fig. 10(A) and (B). The average ESS was 1.35 Pa, while the average normalized LDL concentration was 0.1. The average transmigrated monocytes where 104 cells per mm^2 [Fig. 10(C)]. From the geometry of the arterial segment, it is clear that the curvature affects the distribution of ESS, with high ESS estimated at the regions of small diameter. On the other hand, increased LDL accumulation was found at the region of low ESS. In these regions we also calculated increased migration of monocytes.

Oxidized LDL concentration presents a similar distribution as the LDL concentration. HDL protects LDL molecules from oxidation and thus the oxidation rate of LDL in regions of high HDL concentration is reduced. Finally, macrophages and foam cells had a different distribution from the other

computed variables. This is caused by our assumption that macrophage differentiation depends also on the cytokines concentration which is increased in regions of increased arterial wall thickness and moreover on the baseline macrophages intensity found at the OCT images.

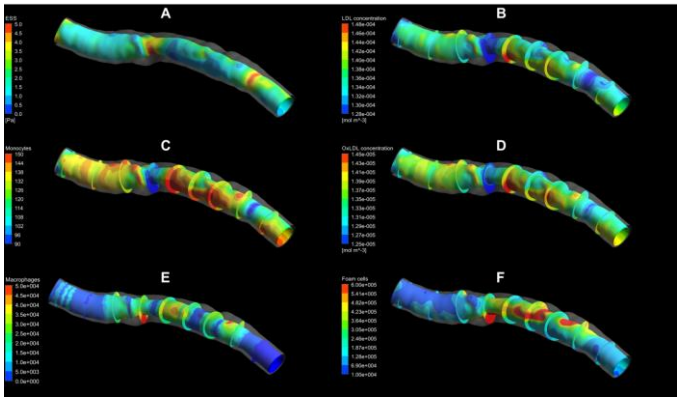

Fig. 10. (A) Endothelial shear stress (ESS) distribution at the luminal surface, (B) normalized subendothelial LDL concentration. (C) Monocytes concentration, (D) Oxidized LDL concentration, (E) Macrophages concentration, (F) Foam cells concentration.

Fig. 11 shows the relation of the computed variables with the plaque area change. It is clear that all the variables have a good correlation and could be used to predict the change in plaque thickness.

As shown in Fig. 11, both ESS and LDL concentration have very strong correlation with fibrotic and fibrofatty plaque components. More specifically, ESS has a negative correlation with change in fibrous and fibrofatty plaque with Pearson correlation about -0.76 and -0.88, respectively. However, ESS does not correlate with necrotic core. On the other hand, LDL concentration has a positive correlation with these variables with Pearson about 0.89 and 0.97, respectively. Finally, the calculated macrophages concentration correlate very well with the follow-up macrophages existence (P=0.038) as well as with necrotic core change (P=0.023). Additionally, foam cells are also related with the follow-up macrophages and necrotic core change (P=0.033 and P=0.02, respectively).

Linear regression analysis was performed to identify possible predictors of plaque change area. First we examine ESS as unique predictor, then we add LDL concentration and in a stepwise approach, we add all computed variables to examine whether the predictive probability is increased. When using only ESS as predictor we observe R^2=0.365 (P=0.029, adjusted R^2=0.307). The addition of LDL concentration in the model leads to a higher correlation R^2=0.368 (P=0.015, adjusted R^2=0.342). The increase of the adjusted R^2 means that adding the second predictor to the model increases the accuracy of the prediction. Finally, we add in the model oxidized LDL, macrophages and foam cells. By theory, we expect that adding more predictors in a linear regression analysis the R^2 will increase. For this reason we use the adjusted value to understand whether the addition of predictors contributes to increased prediction. The results of this model show R^2=0.847 (P=0.009, adjusted R^2=0.738).

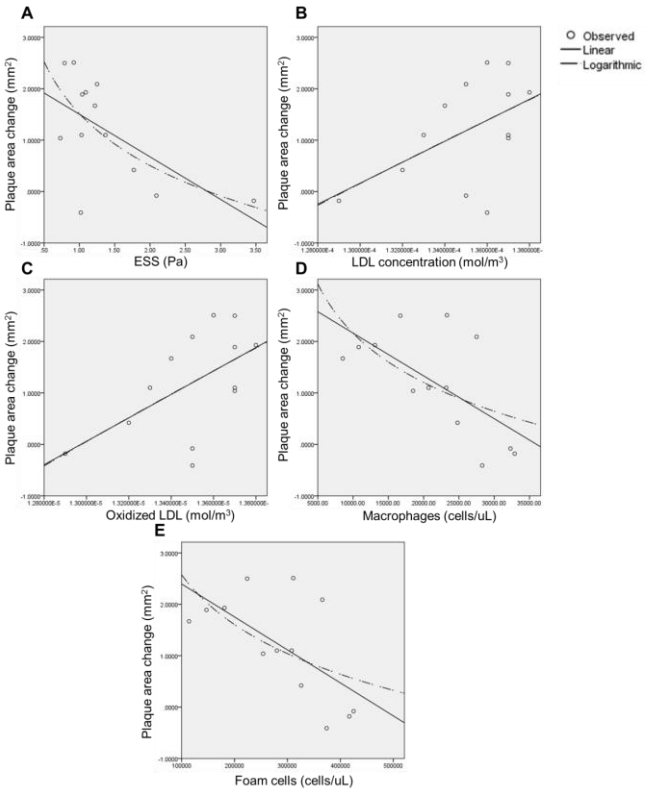

Fig. 11. Relation of plaque area change with the computed variables [ESS, LDL concentration, oxidized LDL, macrophages and foam cells for (A), (B), (C), (D), (E), respectively]. Good correlation is observed for all dependent variables.

IV. Discussion

In the proposed work, we present a mathematical model for multilevel patient specific prediction of plaque growth. More specifically, the multi-level model consists of three discrete levels of modeling: i) blood flow modeling and ESS calculation, ii) LDL and monocytes transport and accumulation into the arterial wall, and iii) plaque growth modeling considering macrophages transformation and foam cells formation. The innovation of this study is: i) the integration of the macrophages transport, ii) the use of HDL concentration and its athero-protective role to LDL oxidation, iii) the use of data observed from animal studies which are conducted for this specific purpose, iv) the model of macrophage differentiation based on the effect of oxidized LDL, and v) the validation of the results using a proof of concept human data with follow-up imaging data.

Several clinical, preclinical and computational studies demonstrated that ESS plays a crucial role to plaque formation. More specifically, regions of low ESS are more prone to exhibit disease progression, where the ESS is low or the flow disturbed [7]. In our study, ESS has a relatively good inverse relation with the change of the plaque area of the arterial segment. Also, regarding the comparison of the ESS in the baseline with the VH follow-up findings, it is shown that ESS is correlated well with change in fibrous and fibrofatty tissue. This finding is in agreement with Goubergrits *et al*. [35], where it was shown that low ESS correlates with regions of fibrous plaque.

Table II
COMPARISON BETWEEN THE CHANGE IN GEOMETRY AND PLAQUE COMPONENTS RECOGNIZED IN VH FRAMES WITH CALCULATED VARIABLES.

Variable		ESS	LDL	Oxidized LDL	Macrophages	Foam cells
% change of plaque area	Pearson	-0.693*	0.804**	0.833**	-0.653*	-0.650*
	P value	0.026	0.005	0.003	0.041	0.041
% change of lumen area	Pearson	0.753*	-0.806**	-0.783**	0.637*	0.664*
	P value	0.012	0.005	0.007	0.047	0.036
% change of necrotic burden	Pearson	-0.459	0.409	0.318	0.622	0.634
	P value	0.253	0.314	0.443	0.023	0.02
% change of calcium plaque	Pearson	-0.03	-0.038	-0.182	-0.035	-0.093
	P value	0.944	0.928	0.666	0.934	0.827
% change of fibrous plaque	Pearson	-0.759*	0.893**	0.929**	-0.790*	-0.773*
	P value	0.029	0.003	0.001	0.020	0.024
% change of fibrofatty plaque	Pearson	-0.876**	0.969**	0.964**	-0.866**	-0.856**
	P value	0.004	0.000	0.000	0.005	0.007
Follow-up macrophages	Pearson	N/A	N/A	N/A	0.579*	0.0592*
	P value				0.038	0.033

Similarly, Chatzizisis *et al*. [2] showed that fibroatheroma is found mainly in low ESS regions in the arterial segment while in Samady *et al*.[7] it was found that high shear stress is significantly correlated with the fibrous and fibrofatty area regression. It seems that for the specific case report, ESS can be used as a predictor for potential regions of plaque progression and especially, for prediction of fibroatheroma increase.

Regarding the LDL accumulation in the arterial wall we find a similar, but inverse, association with plaque area change. This is due to the fact that LDL accumulation is related to ESS. The observed co-localization of low ESS with high subendothelial LDL accumulation is caused mainly by two mechanisms. First, decrease of ESS is caused by slow or stagnant blood flow which results in LDL particles stagnation, which consequently contributes to the phenomenon called concentration polarization, described by the formation of an LDL rich luminal layer adjacent to the endothelium [5, 36]. This increased luminal LDL concentration may increase the diffusion of the molecules and thus the diffusive component of the solute flux from Kedem-Katchalsky equations. Second, according to the relationship between ESS and hydraulic conductivity, we should expect lower transmural velocity and solute flux at low ESS regions. Transmural velocity is a dominant feature of LDL transport in the arterial wall, and the result of reduced transmural velocity is a decrease in the convection of LDL (low efflux) from the subendothelial layer to the outer layers of the arterial wall leading to the relatively augmented subendothelial LDL accumulation. Similar findings were reported in previous studies in human arteries employing an ESS-dependent hydraulic conductivity [13]. Statistical significance is found between LDL concentration and plaque area change which means that low ESS and high LDL concentration can be used to depict regions prone for plaque progression [37-39]. This is in accordance with previously presented results where low ESS and high LDL concentration are independent predictors of disease progression. In the study of Holvoet *et al.* [40], it was found with histological data that lipid concentration is related to plaque growth and reduction of lumen area. The relation of LDL concentration and ESS is in agreement with the experimental study of Meyer *et al*.[41].

Monocytes recruitment, adherence and transport through the endothelial membrane are processes that are involved in atherosclerotic lesion formation. Macrophages are one of the major cell types which are involved at the early stages of the atherosclerotic process. Arterial wall contains resident monocytes; in atherosclerotic lesions the monocytes are usually differentiated into inflammatory macrophages[42]. Oxidized LDL is found to promote the differentiation of monocytes to macrophages and promotes vascular inflammation [43]. The proposed model attempts to describe the mechanism of macrophage differentiation using the oxidized LDL as regulating factor. Oxidized LDL has several forms in the arterial wall. However, in this work we assume only a major substance of oxidized LDL which includes the 7-KC molecule. This approach was chosen because 7-KC is found in large amounts into the oxidized LDL particles, but also there is lack of experimental studies which describe the effect of the different forms of oxidized LDL on macrophage differentiation.

The final step of the multilevel modeling approach is the estimation of macrophages in the arterial wall and the formation of foam cells. Macrophages are responsible for oxidized LDL phagocytosis. The increased phagocytosis of LDL results in the formation of "foam" cells [44]. In our work, we also assume that the differentiation of macrophages depends on the cytokines expression and especially on the concentration of the MIF molecule which is related to existed lesion area as observed in the histological images of our animal studies. In this way the macrophages concentration depends on three factors acting in parallel: i) on oxidized LDL, and ii) on the underlying plaque and iii) on the existence of macrophages. Our results regarding the prediction of macrophages and necrotic core change are of potential clinical value. Both characteristics are considered as markers of plaque vulnerability[45-48] and in this way we might assume that our model can predict vulnerable plaques.

In our simulation foam cells are directly generated by the absorption of oxidized LDL by macrophages. The approach is

simple, but the experimental data of this mechanism are few for developing a complex mathematical model. However, our results show that the presented computational model might be used for prediction of atherosclerotic plaque growth in this specific proof of concept case.

The main limitation of this study is that it has been tested in only one human case. This does not allow making strong conclusions about the accuracy of the model. Moreover, though the current model describes the major mechanisms which underlie atherosclerotic process, several other processes are neglected, such as the role of calcium or the proliferation of the smooth muscle cells. Additionally, another limitation of the current model is that does not include the evolution in time. It is a steady state model, but we plan to include time in our future work. Finally, the presented computational model is based on some assumptions. More specifically, the main relations which are applied mainly as boundary conditions in the proposed mathematical model are based on *in vitro* experimental studies or on animal studies. This means that most of them may not represent the human physiology. However, we perform appropriate fitting to translate the experimental values to human ones in order to overcome this limitation.

V. Conclusions

In this work, we present a multilevel modeling approach, which can be used for prediction of plaque growth. The approach is based on modeling of blood flow, LDL transport as well as macrophages migration and foam cells formation. For the first time, such a computational plaque growth model is tested in human serial imaging data (IVUS-VH and OCT). Our results indicate that a multilevel model offers more capabilities for more accurate prediction of regions potential for plaque growth and even plaque rupture, than simple blood flow modeling and ESS computation.

References

[1] W. H. O. (WHO). *The atlas of heart disease and stroke*. Available: http://www.who.int/cardiovascular_diseases/en/cvd_atlas_16_death_from_stroke.pdf

[2] Y. S. Chatzizisis, M. Jonas, A. U. Coskun, R. Beigel, B. V. Stone, C. Maynard, *et al.*, "Prediction of the localization of high-risk coronary atherosclerotic plaques on the basis of low endothelial shear stress - An intravascular ultrasound and histopathology natural history study," *Circulation*, vol. 117, pp. 993-1002, Feb 26 2008.

[3] J. M. Tarbell, Z. D. Shi, J. Dunn, and H. Jo, "Fluid Mechanics, Arterial Disease, and Gene Expression," *Annual Review of Fluid Mechanics, Vol 46*, vol. 46, pp. 591-614, 2014.

[4] L. M. Cancel and J. M. Tarbell, "The role of mitosis in LDL transport through cultured endothelial cell monolayers," *American Journal of Physiology-Heart and Circulatory Physiology*, vol. 300, pp. H769-H776, Mar 2011.

[5] J. M. Tarbell, "Shear stress and the endothelial transport barrier," *Cardiovascular Research*, vol. 87, pp. 320-330, Jul 15 2010.

[6] P. H. Stone, A. U. Coskun, S. Kinlay, J. J. Popma, M. Sonka, A. Wahle, *et al.*, "Regions of low endothelial shear stress are the sites where coronary plaque progresses and vascular remodelling occurs in humans: an in vivo serial study," *European Heart Journal*, vol. 28, pp. 705-710, Mar 2007.

[7] H. Samady, P. Eshtehardi, M. C. McDaniel, J. Suo, S. S. Dhawan, C. Maynard, *et al.*, "Coronary Artery Wall Shear Stress Is Associated With Progression and Transformation of Atherosclerotic Plaque and Arterial Remodeling in Patients With Coronary Artery Disease," *Circulation*, vol. 124, pp. 779-788, Aug 16 2011.

[8] P. H. Stone, S. Saito, S. Takahashi, Y. Makita, S. Nakamura, T. Kawasaki, *et al.*, "Prediction of Progression of Coronary Artery Disease and Clinical Outcomes Using Vascular Profiling of Endothelial Shear Stress and Arterial Plaque Characteristics The PREDICTION Study," *Circulation*, vol. 126, pp. 172-181, Jul 10 2012.

[9] M. R. Kaazempur-Mofrad, S. Wada, J. G. Myers, and C. R. Ethier, "Mass transport and fluid flow in stenotic arteries: Axisymmetric and asymmetric models," *International Journal of Heat and Mass Transfer*, vol. 48, pp. 4510-4517, Oct 2005.

[10] M. R. Kaazempur-Mofrad and C. R. Ethier, "Mass transport in an anatomically realistic human right coronary artery," *Annals of Biomedical Engineering*, vol. 29, pp. 121-127, Feb 2001.

[11] U. Olgac, V. Kurtcuoglu, and D. Poulikakos, "Computational modeling of coupled blood-wall mass transport of LDL: effects of local wall shear stress," *Am J Physiol Heart Circ Physiol*, vol. 294, pp. H909-19, Feb 2008.

[12] U. Olgac, D. Poulikakos, S. C. Saur, H. Alkadhi, and V. Kurtcuoglu, "Patient-specific three-dimensional simulation of LDL accumulation in a human left coronary artery in its healthy and atherosclerotic states," *American Journal of Physiology-Heart and Circulatory Physiology*, vol. 296, pp. H1969-H1982, Jun 2009.

[13] N. Sun, R. Torii, N. B. Wood, A. D. Hughes, S. A. Thom, and X. Y. Xu, "Computational modeling of LDL and albumin transport in an in vivo CT image-based human right coronary artery," *J Biomech Eng*, vol. 131, p. 021003, Feb 2009.

[14] N. Sun, N. B. Wood, A. D. Hughes, S. A. Thom, and X. Y. Xu, "Fluid-wall modelling of mass transfer in an axisymmetric stenosis: effects of shear-dependent transport properties," *Ann Biomed Eng*, vol. 34, pp. 1119-28, Jul 2006.

[15] N. Sun, N. B. Wood, A. D. Hughes, S. A. Thom, and X. Y. Xu, "Influence of pulsatile flow on LDL transport in the arterial wall," *Ann Biomed Eng*, vol. 35, pp. 1782-90, Oct 2007.

[16] S. Chung and K. Vafai, "Low-density lipoprotein transport within a multi-layered arterial wall-Effect of the atherosclerotic plaque/stenosis," *Journal of Biomechanics*, vol. 46, pp. 574-585, Feb 1 2013.

[17] N. Yang and K. Vafai, "Low-density lipoprotein (LDL) transport in an artery - A simplified analytical solution," *International Journal of Heat and Mass Transfer*, vol. 51, pp. 497-505, Feb 2008.

[18] N. Yang and K. Vafai, "Modeling of low-density lipoprotein (LDL) transport in the artery-effects of hypertension," *International Journal of Heat and Mass Transfer*, vol. 49, pp. 850-867, Mar 2006.

[19] P. Siogkas, A. Sakellarios, T. P. Exarchos, L. Athanasiou, E. Karvounis, K. Stefanou, *et al.*, "Multiscale - Patient-Specific Artery and Atherogenesis Models," *Ieee Transactions on Biomedical Engineering*, vol. 58, pp. 3464-3468, Dec 2011.

[20] A. I. Sakellarios, M. I. Papafaklis, P. Siogkas, L. S. Athanasiou, T. P. Exarchos, K. Stefanou, *et al.*, "Patient-specific computational modeling of subendothelial LDL accumulation in a stenosed right coronary artery: effect of hemodynamic and biological factors," *American Journal of Physiology-Heart and Circulatory Physiology*, vol. 304, pp. H1455-H1470, Jun 2013.

[21] A. I. Sakellarios, P. Siogkas, T. P. Exarchos, K. Stefanou, C. V. Bourantas, L. Athanasiou, *et al.*, "Modelling LDL Accumulation in the case of Endothelial Dysfunction," *Journal of the Serbian Society for Computational Mechanics*, vol. 5, pp. 90-100, 2011.

[22] U. Olgac, J. Knight, D. Poulikakos, S. C. Saur, H. Alkadhi, L. M. Desbiolles, *et al.*, "Computed high concentrations of low-density lipoprotein correlate with plaque locations in human coronary arteries," *Journal of Biomechanics*, vol. 44, pp. 2466-2471, Sep 2 2011.

[23] U. Olgac, V. Kurtcuoglu, and D. Poulikakos, "Computational modeling of coupled blood-wall mass transport of LDL: effects of local wall shear stress (vol 63, pg H915, 2008)," *American Journal of Physiology-Heart and Circulatory Physiology*, vol. 294, pp. H2917-H2917, Jun 2008.

[24] N. Filipovic, M. Rosic, I. Tanaskovic, Z. Milosevic, D. Nikolic, N. Zdravkovic, *et al.*, "ARTreat Project: Three-Dimensional Numerical Simulation of Plaque Formation and Development in the Arteries," *Ieee Transactions on Information Technology in Biomedicine*, vol. 16, pp. 272-278, Mar 2012.

[25] O. Parodi, T. P. Exarchos, P. Marraccini, F. Vozzi, Z. Milosevic, D. Nikolic, *et al.*, "Patient-Specific Prediction of Coronary Plaque Growth From CTA Angiography: A Multiscale Model for Plaque Formation and Progression," *Ieee Transactions on Information Technology in Biomedicine*, vol. 16, pp. 952-965, Sep 2012.

[26] A. I. Sakellarios, P. Bizopoulos, K. Stefanou, L. S. Athanasiou, M. I. Papafaklis, C. V. Bourantas, *et al.*, "A proof-of-concept study for predicting the region of atherosclerotic plaque development based on plaque growth modeling in carotid arteries," *Conf Proc IEEE Eng Med Biol Soc*, vol. 2015, pp. 6552-5, Aug 2015.

[27] L. Raber, M. Taniwaki, S. Zaugg, H. Kelbaek, M. Roffi, L. Holmvang, *et al.*, "Effect of high-intensity statin therapy on atherosclerosis in non-infarct-related coronary arteries (IBIS-4): a serial intravascular ultrasonography study," *European Heart Journal*, vol. 36, pp. 490-500, Feb 21 2015.

[28] C. V. Bourantas, I. C. Kourtis, M. E. Plissiti, D. I. Fotiadis, C. S. Katsouras, M. I. Papafaklis, *et al.*, "A method for 3D reconstruction of coronary arteries using biplane angiography and intravascular ultrasound images," *Computerized Medical Imaging and Graphics*, vol. 29, pp. 597-606, Dec 2005.

[29] N. Solanes, M. Rigol, J. Ramirez, J. Segales, M. Roque, J. M. Marimon, *et al.*, "Histological basis of the porcine femoral artery for vascular research," *Anatomia Histologia Embryologia*, vol. 34, pp. 105-111, Apr 2005.

[30] S. T. Kunitake, M. R. Jarvis, R. L. Hamilton, and J. P. Kane, "Binding of Transition-Metals by Apolipoprotein-a-I-Containing Plasma-Lipoproteins - Inhibition of Oxidation of Low-Density Lipoproteins," in *Proceedings of the National Academy of Sciences of the United States of America*, 1992, pp. 6993-6997.

[31] A. Sakellarios, P. Siogkas, L. Athanasiou, T. P. Exarchos, M. I. Papafaklis, C. Bourantas, *et al.*, "Three-dimensional modeling of oxidized-LDL accumulation and HDL mass transport in a coronary artery: A proof-of-concept study for predicting the region of atherosclerotic plaque development," in *International Conference of the IEEE Engineering in Medicine and Biology Society, EMBS*, Osaka, 2013.

[32] J. M. Hayden, L. Brachova, K. Higgins, L. Obermiller, A. Sevanian, S. Khandrika, *et al.*, "Induction of monocyte differentiation and foam cell formation in vitro by 7-ketocholesterol," *Journal of Lipid Research*, vol. 43, pp. 26-35, Jan 2002.

[33] O. Kedem and A. Katchalsky, "Thermodynamic analysis of the permeability of biological membranes to non-electrolytes," *Biochim Biophys Acta*, vol. 27, pp. 229-46, Feb 1958.

[34] J. K. Tsou, R. M. Gower, H. J. Ting, U. Y. Schaff, M. F. Insana, A. G. Passerini, *et al.*, "Spatial regulation of inflammation by human aortic endothelial cells in a linear gradient of shear stress," *Microcirculation*, vol. 15, pp. 311-323, 2008.

[35] L. Goubergrits, K. Affeld, J. Fernandez-Britto, and L. Falcon, "Atherosclerosis and flow in carotid arteries with authentic geometries," *Biorheology*, vol. 39, pp. 519-524, 2002.

[36] J. M. Tarbell, "Mass transport in arteries and the localization of atherosclerosis," *Annual Review of Biomedical Engineering*, vol. 5, pp. 79-118, 2003.

[37] A. Sakellarios, C. V. Bourantas, S. L. Papadopoulou, Z. Tsirka, T. de Vries, P. H. Kitslaar, *et al.*, "Prediction of atherosclerotic disease progression using LDL transport modelling: a serial computed tomographic coronary angiographic study," *Eur Heart J Cardiovasc Imaging*, Mar 16 2016.

[38] C. Bourantas, S. Papadopoulou, P. Serruys, A. Sakellarios, P. Kitslaar, P. Bizopoulos, *et al.*, "Non-Invasive Prediction of Atherosclerotic Progression: Analysis from the PROSPECT-MSCT study," *Jacc-Cardiovascular Imaging*, vol. In Press, 2015.

[39] A. I. Sakellarios, P. Bizopoulos, M. I. Papafaklis, L. Athanasiou, T. Exarchos, C. V. Bourantas, *et al.*, "Natural History of Carotid Atherosclerosis in Relation to the Hemodynamic Environment: A Low-Density Lipoprotein Transport Modeling Study With Serial Magnetic Resonance Imaging in Humans," *Angiology*, Apr 14 2016.

[40] P. Holvoet, G. Theilmeier, B. Shivalkar, W. Flameng, and D. Collen, "LDL hypercholesterolemia is associated with accumulation of oxidized LDL, atherosclerotic plaque growth, and compensatory vessel enlargement in coronary arteries of miniature pigs," *Arteriosclerosis Thrombosis and Vascular Biology*, vol. 18, pp. 415-422, Mar 1998.

[41] G. Meyer, R. Merval, and A. Tedgui, "Effects of pressure-induced stretch and convection on low-density lipoprotein and albumin uptake in the rabbit aortic wall," *Circ Res*, vol. 79, pp. 532-40, Sep 1996.

[42] K. Ley, Y. I. Miller, and C. C. Hedrick, "Monocyte and Macrophage Dynamics During Atherogenesis," *Arteriosclerosis Thrombosis and Vascular Biology*, vol. 31, pp. 1506-1516, Jul 2011.

[43] J. Frostegard, J. Nilsson, A. Haegerstrand, A. Hamsten, H. Wigzell, and M. Gidlund, "Oxidized Low-Density Lipoprotein Induces Differentiation and Adhesion of Human Monocytes and the Monocytic Cell-Line U937," *Proceedings of the National Academy of Sciences of the United States of America*, vol. 87, pp. 904-908, Feb 1990.

[44] X. H. Yu, Y. C. Fu, D. W. Zhang, K. Yin, and C. K. Tang, "Foam cells in atherosclerosis," *Clinica Chimica Acta*, vol. 424, pp. 245-252, Sep 23 2013.

[45] M. J. Davies, P. D. Richardson, N. Woolf, D. R. Katz, and J. Mann, "Risk of Thrombosis in Human Atherosclerotic Plaques - Role of Extracellular Lipid, Macrophage, and Smooth-Muscle Cell Content," *British Heart Journal*, vol. 69, pp. 377-381, May 1993.

[46] P. R. Moreno, E. Falk, I. F. Palacios, J. B. Newell, V. Fuster, and J. T. Fallon, "Macrophage Infiltration in Acute Coronary Syndromes - Implications for Plaque Rupture," *Circulation*, vol. 90, pp. 775-778, Aug 1994.

[47] A. V. Finn, M. Nakano, J. Narula, F. D. Kolodgie, and R. Virmani, "Concept of Vulnerable/Unstable Plaque," *Arteriosclerosis Thrombosis and Vascular Biology*, vol. 30, pp. 1282-1292, Jul 2010.

[48] A. Seneviratne, M. Hulsmans, P. Holvoet, and C. Monaco, "Biomechanical factors and macrophages in plaque stability," *Cardiovascular Research*, vol. 99, pp. 284-293, Jul 15 2013.